

# Engineering Notes

ENGINEERING NOTES are short manuscripts describing new developments or important results of a preliminary nature. These Notes should not exceed 2500 words (where a figure or table counts as 200 words). Following informal review by the Editors, they may be published within a few months of the date of receipt. Style requirements are the same as for regular contributions (see inside back cover).

## Unified Approximation for Nonparabolic Drag Polars

Lance W. Traub\*

Embry-Riddle Aeronautical University,  
Prescott, Arizona 86301

DOI: 10.2514/1.28646

### Introduction

THE drag polar, the variation of drag coefficient ( $C_d$  or  $C_D$ ) with lift coefficient ( $C_l$  or  $C_L$ ), is often approximated with an expression of the form [1,2]

$$C_d = C_{d0} + k_p C_l^2 \quad (\text{airfoil}) \quad (1a)$$

$$C_D = C_{D0} + k_{p+i} C_L^2 \quad (\text{wing}) \quad (1b)$$

where, by convention (excluding the  $k$  term), uppercase subscripts apply to wings and lowercase subscripts apply to airfoils. The first term on the right-hand side is the drag coefficient at zero lift and the second term represents the contribution of pressure drag ( $k_p C_l^2$  for the airfoil) or pressure and induced (vortex) drag ( $k_{p+i} C_L^2$  for the wing). For wings, both the pressure component of the profile drag coefficient  $k_p C_L^2$  and the planform-dependent induced drag coefficient  $k_i C_L^2$  vary with the square of the lift coefficient. This makes their separation difficult [thus the combination  $k_{p+i}$  parameter in Eq. (1b)]. Equations (1a) and (1b) are used as an approximation in performance estimates for preliminary design, as well as for interpretation and quantification of experimental and computational data. The form of Eq. (1) implies that the minimum drag of the configuration (airfoil or wing) occurs at zero lift. This is generally true for symmetrical airfoils or wings. For cambered airfoils or cambered section wings, a more representative approximation is of the form

$$C_d = C_{d\min} + k_p (C_l - C_{lmd})^2 \quad (\text{airfoil}) \quad (2a)$$

$$C_D = C_{D\min} + k_{p+i} (C_L - C_{Lmd})^2 \quad (\text{wing}) \quad (2b)$$

$$C_D = C_{d\min} + k_p (C_L - C_{lmd})^2 + k_i C_L^2 \quad (\text{wing}) \quad (2c)$$

where  $C_{d\min}$  is the minimum airfoil drag coefficient,  $C_{D\min}$  is the minimum wing drag coefficient, and  $C_{lmd}$  and  $C_{Lmd}$  are the drag coefficients at which minimum drag occurs for the airfoil and wing, respectively. Equation (2c) is also used for drag polar analysis of

wings and includes contributions from the airfoil and wing drag polars. In Eq. (2c),  $k_p$  is determined from airfoil data. Equations (2b) and (2c) are equivalent and yield similar estimates ( $k_{p+i} = k_p + k_i$ ) when used for polar analysis, however, Eq. (2b) does not require any knowledge of the airfoil drag polar.

The functional form of Eqs. (2a) and (2b) effectively shifts the polar so that it achieves symmetry around the vertical axis. For wings,  $k_i$  in Eqs. (1) or (2) is often referred to as the induced efficiency factor, which may be expressed as

$$k_i = \frac{1}{\pi AR e} \quad (3)$$

where AR is the aspect ratio and  $e$  is the Oswald (or span) efficiency factor. For either an airfoil or wing, minimization of  $k_p$  or  $k_{p+i}$  is reflected in increased efficiency. The accuracy of Eq. (2) is dependent on representative determination of  $C_{lmd}$  or  $C_{Lmd}$ , which may be difficult. It is also implicitly assumed that the drag polar can be represented by a single parabolic expression. However, this is not necessarily the case. Laminar flow sections show evidence of a region of almost constant drag, the drag bucket, followed by a drag rise (although this is typically difficult to achieve and maintain due to contamination and structural vibration, perhaps requiring active flow control). This form of drag distribution is not amenable to modeling using a single parabolic form. Higher-order polynomials may be used to approximate the polar; however, they may show oscillations and do not work well for sudden discontinuities. In addition, the correct mathematical representation of the physics is lost.

In this Note, a unified drag polar approximation is presented that allows for modeling of apparently nonparabolic polars with discontinuities. The approximation should prove useful for performance studies and extraction or quantification of aerodynamic characteristics.

### Theoretical Development

To establish if there are consistently identifiable characteristics in the linearized polars [drag coefficient plotted as a function of  $C_l^2$  or  $(C_l - C_{lmd})^2$  for airfoils or  $C_L^2$  and  $(C_L - C_{Lmd})^2$  for wings] of cambered airfoils and wings, several polars were analyzed [3,4]. The analysis showed that most polars appear to be composed of essentially two parabolic sections that, when linearized, are delineated by changes of slope of the linear sections of the polar. Typical polars are presented in Figs. 1–3. Thus, a suitable approximation for this form of polar may be described by a function consisting of two fits that each contribute to the function only in the domain in which it is representative. Consequently, an expression of the form

$$C_d = \varepsilon [C_{d01} + k_{p1} (C_l - C_{lmd})^2] + (1 - \varepsilon) [C_{d02} + k_{p2} (C_l - C_{lmd})^2] \quad (\text{airfoil}) \quad (4a)$$

$$C_D = \varepsilon [C_{D01} + k_{(p+i)1} (C_L - C_{Lmd})^2] + (1 - \varepsilon) [C_{D02} + k_{(p+i)2} (C_L - C_{Lmd})^2] \quad (\text{wing}) \quad (4b)$$

should be suitable. The first term in braces is a parabolic approximation corresponding to a curve fit of the first slope of the linearized polar (which would encompass the minimum drag region)

Received 31 October 2006; revision received 28 November 2006; accepted for publication 18 November 2006. Copyright © 2006 by Lance W. Traub. Published by the American Institute of Aeronautics and Astronautics, Inc., with permission. Copies of this paper may be made for personal or internal use, on condition that the copier pay the \$10.00 per-copy fee to the Copyright Clearance Center, Inc., 222 Rosewood Drive, Danvers, MA 01923; include the code 10.2514/1.28646 in correspondence with the CCC.

\*Associate Professor, Aerospace Engineering Department.

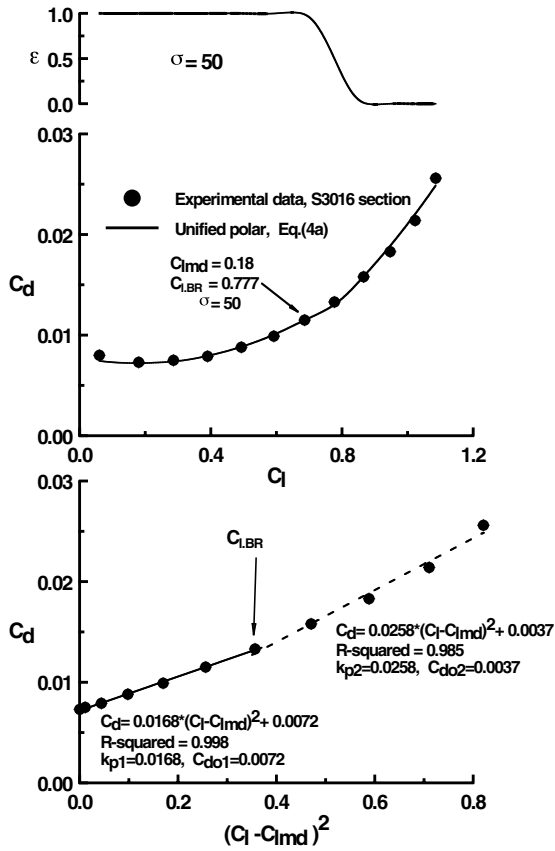


Fig. 1 Experimental drag polar showing unified curve-fit approach for the S3016 airfoil profile [4].

and the second term describes the region of drag rise at higher lift coefficients. The weighing function  $\varepsilon$  is used to assign the domain of the parabolic fits; this function should vary from one to zero. A formulation for the weighing function with the necessary behavior is given by

$$\varepsilon = \frac{1}{1 + e^{\sigma(C_l - C_{lBR})}} \quad (\text{airfoil}) \quad \text{and} \quad \varepsilon = \frac{1}{1 + e^{\sigma(C_L - C_{LBR})}} \quad (\text{wing}) \quad (5)$$

where  $C_{lBR}$  and  $C_{LBR}$  are the lift coefficients at which the linearized polar changes slope and may also be selected by looking at the drag polar for any points of discontinuity;  $\sigma$  determines the rate at which the value of  $\varepsilon$  changes from one to zero. The larger the value of  $\sigma$ , the more rapidly  $\varepsilon$  varies from one to zero (i.e.,  $\sigma$  is a magnification factor).

### Implementation

Fitting Eqs. (4a) or (4b) to a data set may be accomplished using the following steps (which are itemized for an airfoil polar, but the process would be identical for a wing, except that all terms and coefficients would pertain to the wing's polar):

1. Select  $C_{lmd}$  from observation of the drag polar.  $C_{lmd}$  should correspond to a point that yields the best symmetry (i.e., a point near the middle of the drag bucket or arc in the minimum drag region).
2. Plot the linearized drag polar based upon Eq. (2a) [i.e.,  $C_d$  vs  $(C_l - C_{lmd})^2$ ].
3. Look for slope changes (linearized drag polar) or curve discontinuities (drag polar). The lift coefficient for the observed change corresponds to  $C_{lBR}$ . If no slope change is perceptible, then Eq. (2a) [as opposed to (4a)] can be used to approximate the drag polar.
4. Select  $C_{lBR}$ .
5. Fit linear regressions to the linearized drag polar data, one for  $C_l \geq C_{lBR}$  (second regression) and the other for  $C_{lBR} \geq C_l$  (first

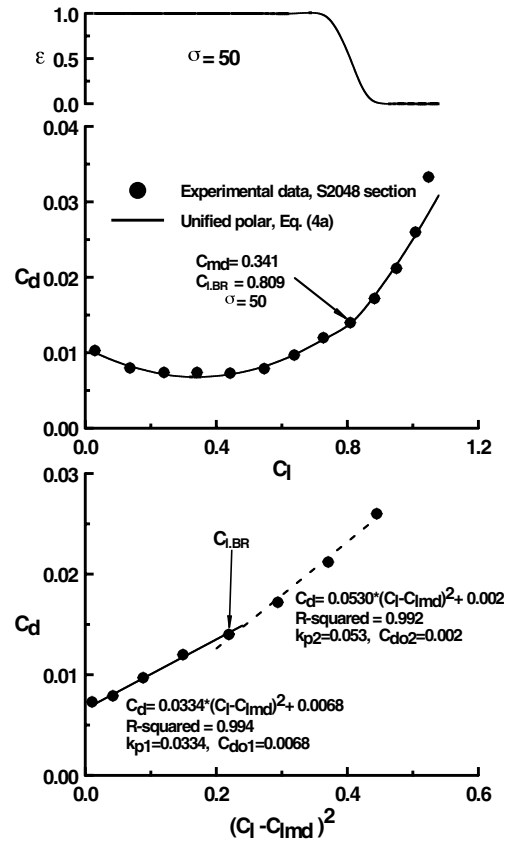


Fig. 2 Experimental drag polar showing unified curve-fit approach for the S2048 airfoil profile [4].

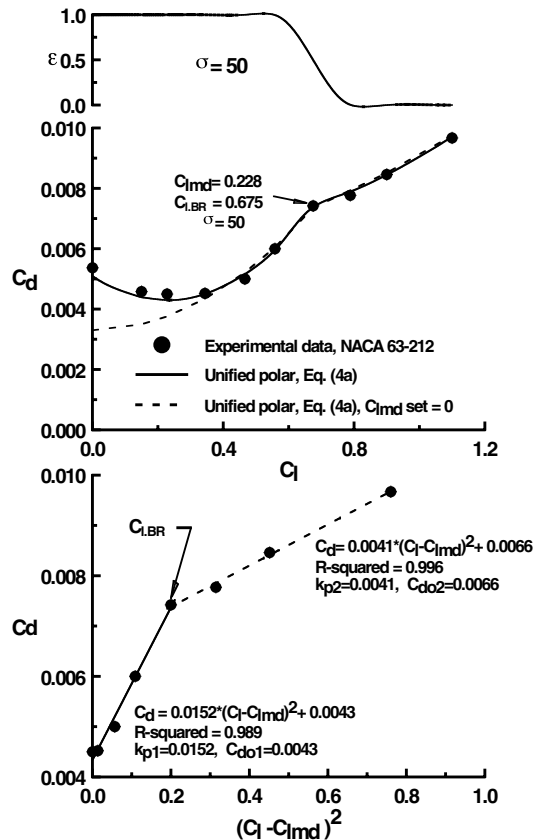


Fig. 3 Experimental drag polar showing unified curve-fit approach for the NACA 63-212 airfoil profile [3].

**Table 1 Performance parameter estimates using Eqs. (9) and (10)**

Section	$C_l/C_{d_{\max}}$ , Eq. (10)	$C_l/C_{d_{\max}}$ , experiment [4]	% difference	$C_{l(l/d \max)}$ , Eq. (9)	$C_{l(l/d \max)}$ , experiment [4]	% difference
S3016	59.65	59.79	−0.23	0.679	0.686	−1.02
S2048	66.60	69.11	−3.61	0.566	0.546	3.66

regression). The slope of these lines is equal to  $k_p$  (or  $k_{p+i}$  if a wing polar was analyzed).

6. In each linear regression, include  $C_{lBR}$  as the last point for the first regression and the first point for the second regression. Adjust the number of points to cover as much of the polar as possible (maximum number of points), while also adjusting the number to maximize the goodness of fit  $r^2$  for both regressions.

7. Changing  $C_{lmd}$  slightly may maximize  $r^2$ .

Figures 1–3 show experimental section data [3,4] for three cambered profiles. The lower inset presents the linearized polar for the section, whereas the middle inset shows the polar. Also included in the middle inset is a representation of the polar using the unified polar methodology described previously. The section data in Fig. 3 are for a laminar flow profile. Extensive regions of laminar flow are reflected in the presence of the drag bucket. Although difficult to achieve in actual flight, this polar form represents a challenging case for a continuous curve fit.

The methodology presented previously was used to fit linear regressions to the low and high lift coefficient regions of the polar curves, as may be seen in the figures. The discontinuity in the slopes of the linearized polars is clearly shown; as is their correspondence to slope changes in the drag polar (middle inset figure), denoted by  $C_{lBR}$ . The top inset in Figs. 1–3 shows the weighing function  $\varepsilon$ . A value of  $\varepsilon = 1$  indicates that the low  $C_l$  linearized polar fit contributes exclusively in Eq. (4a), whereas  $\varepsilon = 0$  shows that the high  $C_l$  linearized polar fit is the only contributor. In the vicinity of  $C_{lBR}$ , a mix of the two fits is used.

The figures clearly show that the unified polar approximation, Eq. (4a), shows excellent fit to the experimental data. Although polars similar to that shown in Fig. 3 are seldom seen in flight vehicles, it is encouraging that Eq. (4a) still holds for this polar form.

Figure 3 also shows a fit to the experimental data using Eq. (4a) with  $C_{lmd} = 0$ , which is analogous to using Eq. (1) as the polar expression in the unified approach. As may be seen, the low-drag region is poorly approximated, because  $C_{lmd}$  is set to zero. Nonetheless, Eq. (1) is often used in aircraft analysis for simplicity and due to difficulties in estimating  $C_{lmd}$ .

The present formulation [Eq. (4b)] does not separate the wing lift-dependent drag coefficient into its sectional pressure and induced drag components. As mentioned, this is difficult, because both components show a lift-coefficient-squared dependency. A decomposition of  $k_{p+i}$  into  $k_p$  and  $k_i$  for cambered wings may be determined as follows. Differentiate Eq. (2c) with respect to  $C_L$  and set equal to zero. The  $C_L$  is then the lift coefficient at which minimum drag occurs,  $C_{Lmd}$ , giving

$$C_D/C_L = 0 = 2k_p(C_{Lmd} - C_{lmd}) + 2k_i C_{Lmd}$$

solving for  $k_i/k_p$  yields

$$\frac{k_i}{k_p} = \frac{C_{lmd}}{C_{Lmd}} - 1$$

using this result and the slope of the linearized polar given by Eq. (4b),  $k_{p+i}$ , gives

$$k_p = k_{p+i} \left( \frac{C_{Lmd}}{C_{lmd}} \right) \quad \text{and} \quad k_i = k_{p+i} \left( 1 - \frac{C_{Lmd}}{C_{lmd}} \right) \quad (6)$$

Note that Eq. (6) requires accurate estimates of the airfoil minimum drag coefficient  $C_{lmd}$ , as well as the wing minimum drag coefficient  $C_{Lmd}$ . Equation (6) is not valid for symmetrical airfoil sections. The sectional and finite wing data should be collected at similar test conditions (e.g., Reynolds number).

Performance analysis approximating the drag polar using Eq. (1b) shows that the maximum  $C_L/C_D$  of an aircraft is given by [5]

$$(C_L/C_D)_{\max} = \frac{1}{2} \sqrt{\frac{1}{C_{D0} \times k_{p+i}}} \quad (7)$$

This expression is used for estimates of maximum range for propeller aircraft and endurance for turbojet aircraft. However, it is not necessarily valid for aircraft with significantly cambered wing sections. An expression for a wing with camber may be developed. It is necessary to minimize

$$\frac{C_D}{C_L} = \frac{C_{D\min} + k_{p+i}(C_L - C_{Lmd})^2}{C_L} \quad (8)$$

which is achieved by setting  $dC_D/dC_L = 0$  and solving for  $C_L$ , which is then equal to the lift coefficient for  $(C_L/C_D)_{\max}$  [i.e.,  $C_{L(L/D \max)}$ ]. Performing the differentiation and solving gives

$$C_{L(L/D \max)} = \sqrt{\frac{C_{D\min}}{k_{p+i}} + C_{Lmd}^2} \quad (9)$$

The maximum  $C_L/C_D$  is then determined from

$$\left( \frac{C_L}{C_D} \right)_{\max} = \frac{\sqrt{[C_{D\min}/(k_{p+i})] + C_{Lmd}^2}}{C_{D\min} + k_{p+i}(C_{L(L/D \max)} - C_{Lmd})^2} \quad (10)$$

Equations (9) and (10) may also be used for airfoil sections; all parameters and coefficients (replace with lowercase subscripts and replace  $k_{p+i}$  with  $k_p$ ) then relate to the airfoil polar. Evaluation of Eqs. (9) and (10) for the experimental airfoil data given in Figs. 1 and 2 is shown in Table 1.

The computations shown in Table 1 show encouraging agreement with the experimental data.

## Conclusions

A methodology for approximating the drag polar of cambered airfoils and wings is presented. The implementation uses two curve fits of the linearized polar to approximate low- and high-loading conditions. A weighing function is used to combine the expressions. Application of the weighed curve fits to experimental data showed encouraging agreement. Expressions are also derived for cambered airfoils and wings for the lift coefficient at which the maximum lift-to-drag ratio occurs, as well as the maximum lift-to-drag ratio. Preliminary correlations of these expressions with experimental data show good agreement.

## References

- [1] McCormick, B. W., *Aerodynamics, Aeronomics and Flight Mechanics*, Wiley, New York, 2nd ed., 1995, p. 174.
- [2] Houghton, E. L., and Carpenter, P. W., *Aerodynamics for Engineering Students*, 5th ed., Butterworth-Heinemann, Oxford, 2003, p. 44.
- [3] Abbott, I. H., and Von Doenhoff, A. E., *Theory of Wing Sections*, Dover, New York, 1959, p. 521.
- [4] Anon., *Airfoil Database* [online database], Nihon University Aero Student Group (NASG), <http://www.nasg.com/afdb/index-e.phtml> [retrieved 15 Oct. 2006].
- [5] Anderson, J. D., Jr., *Aircraft Performance and Design*, McGraw-Hill, New York, 1999, pp. 213–215.